PHYSICAL REVIEW C **72**, 011304(R) (2005)

Evidence for oblate structure in ^{186}Pb

J. Pakarinen,[1,*] I. G. Darby,[2] S. Eeckhaudt,[1] T. Enqvist,[1] T. Grahn,[1] P. T. Greenlees,[1] V. Hellemans,[3] K. Heyde,[3] F. Johnston-Theasby,[4] P. Jones,[1] R. Julin,[1] S. Juutinen,[1] H. Kettunen,[1] M. Leino,[1] A.-P. Leppänen,[1] P. Nieminen,[5] M. Nyman,[1] R. D. Page,[2] P. M. Raddon,[4] P. Rahkila,[1] C. Scholey,[1] J. Uusitalo,[1] and R. Wadsworth[4]

[1]*Department of Physics, University of Jyväskylä, P.O. Box 35, FI-40014, Jyväskylä, Finland*

[2]*Department of Physics, Oliver Lodge Laboratory, University of Liverpool, Liverpool L69 7ZE, United Kingdom*

[3]*Department of Subatomic and Radiation Physics, Proeftuinstraat, 86 B-9000 Gent, Belgium*

[4]*Department of Physics, University of York, Heslington, York Y01 5DD, United Kingdom*

[5]*Department of Nuclear Physics, The Australian National University, Canberra, ACT 0200, Australia*

(Received 14 April 2005; published 29 July 2005)

In-beam $\gamma\gamma$ coincidence data have been collected for ^{186}Pb by combining the JUROGAM Ge-detector array and the GREAT spectrometer with the RITU gas-filled recoil separator for recoil-decay tagging measurements. In addition to the known prolate yrast band in ^{186}Pb, these data have enabled a new low-lying side band to be identified. Based on the analysis of its decay pattern and comparison with Interacting Boson Model (IBM) calculations, the new band is associated with an oblate shape.

DOI: 10.1103/PhysRevC.72.011304 PACS number(s): 27.70.+q, 21.10.Re, 23.20.Lv, 25.70.Gh

In Pb isotopes close to the neutron midshell at $N = 104$, experimental evidence for shape coexisting configurations and associated collective bands has been observed. These structures intrude down to energies close to the spherical ground state and can be associated with intruder 2p–2h and 4p–4h proton shell-model excitations across the $Z = 82$ energy gap [1–5]. Calculations using the deformed mean-field approach, essentially equivalent to the shell-model method, reveal three different shapes (spherical, oblate, and prolate configurations). It remains a challenge for both theoretical and experimental studies to obtain a consistent and detailed description of all the observed phenomena.

In α-decay studies, the first two excited states of the midshell nucleus ^{186}Pb were observed to be 0^+ states [6]. On the basis of α-decay hindrance factors, the 532(21) keV 0_2^+ state was associated with a mainly π(2p–2h) configuration, whereas the 650(23) keV 0_3^+ state was associated with a π(4p–4h) configuration. Consequently, together with the spherical ground state, the three 0^+ states with largely different structures establish a unique shape-triplet in ^{186}Pb.

The 650 keV 0_3^+ state was assumed to be the band head of a collective yrast band that, because of similarities with yrast bands in Hg and Pt isotones, has been assigned to a prolate shape [7–9]. As pointed out in Ref. [6], in order to verify the conclusions drawn from the α-decay studies, it is very important to observe a second, nonyrast collective band of oblate character also. The observation of such a band should shed light on shape mixing and the evolution of shape at higher spin.

To date, collective yrast bands have been identified in the four even–even isotopes $^{182-188}$Pb [7,8,10,11]. In these nuclei, the 0^+ band head is bypassed owing to the competing high-energy $E2$ transition from the first excited 2^+ state to the spherical ground state. Similar yrast bands have been observed in even–even Hg and Pt isotopes with $100 \leqslant N \leqslant 108$ [1,5] and recently in ^{190}Po [12]. All these bands can be associated with prolate intrinsic structure by using a deformed mean-field approach, at least for the higher-spin members.

In addition to the lowest 532 keV 0_2^+ state in ^{186}Pb, a systematic lowering of the first excited 0^+ state in the even–even $^{188-202}$Pb isotopes [13] has been observed. Evidence for the microscopic nature of these states comes, for example, from a low-spin sequence of nonyrast states in ^{196}Pb that can be described as a π(2p–2h) shell-model intruder excitation [14]. However, so far ^{188}Pb is the only Pb isotope for which a well-developed nonyrast collective band has been observed that may well be indicative of the oblate minimum [15]. Yrast bands associated with oblate intruder structures have also been observed in ^{192}Po, ^{194}Po, and ^{198}Rn nuclei [5].

The level spacing in all the observed oblate bands is larger than that of the prolate bands. Therefore, in spite of the low energy of the oblate 0^+ state in ^{186}Pb, the oblate band is expected to lie well above the yrast line and therefore to be weakly populated in fusion-evaporation reactions. The production cross section of ^{186}Pb in available fusion-evaporation reactions is only of the order of 100 μb, and thus tagging techniques are needed to select γ rays emitted by ^{186}Pb. Owing to the relatively long half-life of 4.8 s for the ^{186}Pb α decay, it has so far been difficult to employ the recoil-decay tagging (RDT) [16,17] method for this nucleus. Moreover, a high-efficiency Ge-detector array must be available to obtain $\gamma\gamma$ coincidence information, which is needed for the identification of the nonyrast states. All these factors mean that previous attempts to identify the low-lying oblate intruder band in ^{186}Pb have failed. New spectrometer systems combined with the upgraded RITU gas-filled recoil separator [18] at the Accelerator Laboratory of the University of Jyväskylä (JYFL) have made it possible to perform a successful RDT $\gamma\gamma$ coincidence experiment for ^{186}Pb.

A beam of ^{83}Kr ions was accelerated to an energy of 355 MeV by the K130 cyclotron and used to populate excited

*Corresponding author: janne.pakarinen@phys.jyu.fi

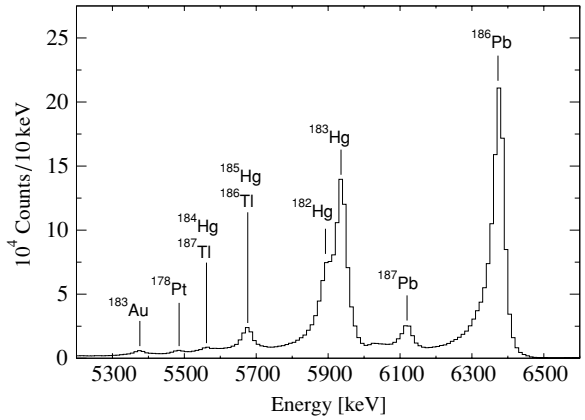

FIG. 1. Energy spectrum of α particles from the ^{83}Kr+^{106}Pd reaction measured in the DSSSDs of the GREAT spectrometer.

states of ^{186}Pb via the ^{106}Pd(^{83}Kr,3n)^{186}Pb reaction. The ^{106}Pd target was a metallic foil of thickness 1 mg/cm^2 and 98.5% isotopic enrichment.

Prompt γ rays were detected at the target position of RITU by the JUROGAM Ge-detector array consisting of 33 EUROGAM Phase 1 [19] and 9 GASP-type [20] Compton suppressed Ge detectors. The beam intensity was limited to 6 pnA by the Ge detector counting rates. The detectors were distributed over six angular positions with respect to the beam direction with five of them at 158°, ten at 134°, ten at 108°, five at 94°, five at 86° and seven at 72°. The total photo peak efficiency of the JUROGAM array for 1332 keV γ rays was 4.1%.

Fusion-evaporation residues were separated from primary and scattered beams and other reaction products by use of the gas-filled recoil separator RITU. The transmission of RITU for the Pb residues in the present experiment was estimated to be 30%. The GREAT spectrometer [21] was employed at the focal plane of RITU. In the GREAT spectrometer fusion-evaporation residues and their α decay were detected by two double-sided silicon strip detectors (DSSSDs) mounted side by side. The strip pitch of each DSSSD was 1 mm in both directions, giving a total of 4800 pixels. A transmission multiwire proportional counter upstream of the DSSSDs was used to obtain energy loss and time-of-flight information for the recoils. A box of 28 PIN diodes was used to detect α particles that escaped from the DSSSDs.

Data were collected by using the new total data readout system [22]. It operates without a hardware trigger and is designed to minimize dead time in the acquisition process. All detector electronics channels run independently and are associated in software, the data words all being time-stamped from a global 100 MHz clock.

The resulting α-particle energy spectrum is shown in Fig. 1. During 151 h of effective beam time, a total of $\sim$10^6 ^{186}Pb α decays were recorded in the 6.38 MeV peak, giving an estimated cross section of 185 μb for the ^{106}Pd(^{83}Kr,3n)^{186}Pb reaction.

The temporal and spatial correlation for RDT were performed with the GRAIN software package [23]. Prompt γ rays observed in coincidence with a recoil followed by a subsequent ^{186}Pb α decay in the same pixel in the GREAT strip detectors within 15 s (approximately three half-lives of ^{186}Pb) were selected in the data analysis. Even with such a long correlation time the high granularity of the GREAT DSSSDs allowed the recoils corresponding to ^{186}Pb to be extracted. The analysis of the data was completed with the RADWARE software package [24].

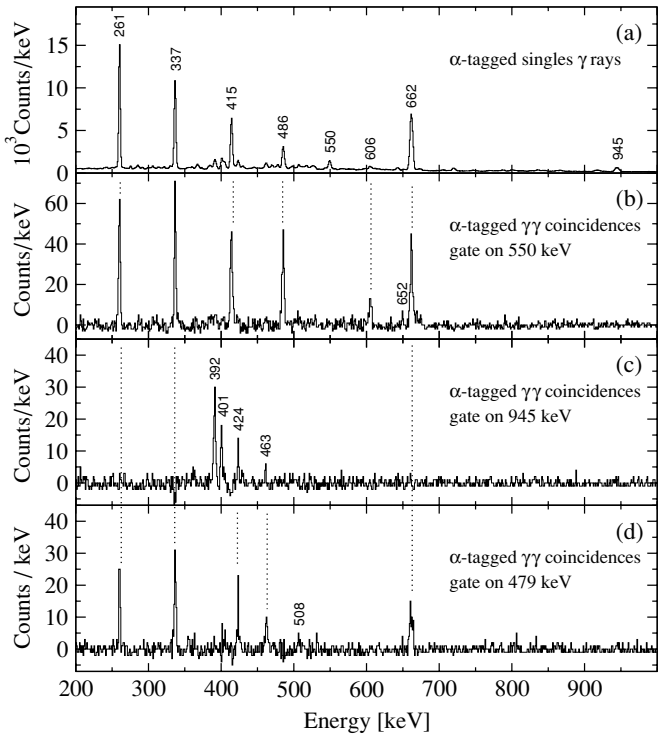

FIG. 2. (a) Singles γ-ray energy spectrum gated with fusion-evaporation residues and tagged with ^{186}Pb α decays. (b), (c), and (d) Recoil-gated, α-tagged $\gamma\gamma$ coincidence spectra with a gate on the 550, 945, and 479 keV transitions, respectively.

The spectrum of recoil-gated prompt γ rays is dominated by γ rays originating from ^{187}Tl and ^{186}Hg produced via pn and 2pn channels, respectively. From recoil-gated data, cross-section estimates of 250 μb and 270 μb were deduced for these reactions, respectively. Figure 2(a) shows the spectrum of singles γ rays gated by recoils and tagged with ^{186}Pb α decays. This spectrum is dominated by transitions of the known prolate yrast band and the $2_1^+ \rightarrow 0_1^+$ transition in ^{186}Pb, but it also reveals other peaks of lower intensity.

The high efficiency of the JUROGAM array allowed the collection of sufficient RDT $\gamma\gamma$ coincidence events to place a large number of nonyrast transitions into a level scheme. Sample coincidence spectra are shown in Figs. 2(b)–(d). Based on the analysis of coincidence relations, the partial level scheme shown in Fig. 3 was constructed. Because of deorientation of recoiling ions [25] and overlapping transition energies, information for spin assignments from γ-ray angular distributions was difficult to obtain, especially at low spin. Experimental information concerning the observed γ-ray transitions is summarized in Table I. R is the ratio of α-tagged singles γ-ray intensities between detectors at 158° (ring 1) and 94°+86° (rings 4+5). For a known stretched, pure $E2$

TABLE I. Measured γ-ray transitions; γ-ray energy, relative intensity, (tentatively) assigned spins, and multipolarity information are listed.

E_γ (keV)	$I_{\rm rel}$	$I_i \rightarrow I_f$	R
662.2(1)	100(6)	$2_1^+ \rightarrow 0_1^+$	1.0(2)
260.6(1)	79(8)	$4_1^+ \rightarrow 2_1^+$	0.9(2)
337.1(1)	74(7)	$6_1^+ \rightarrow 4_1^+$	1.1(2)
414.8(1)	56(5)	$8_1^+ \rightarrow 6_1^+$	—
485.8(5)	28(3)	$10_1^+ \rightarrow 8_1^+$	1.4(4)
549.6(6)	13.4(9)	$12_1^+ \rightarrow 10_1^+$	1.3(4)
605.6(8)	7.1(5)	$(14_1^+) \rightarrow 12_1^+$	—
652.2(2)	2.2(2)	$(16_1^+) \rightarrow (14_1^+)$	—
945.2(3)	5.1(6)	$(2_2^+) \rightarrow 0_1^+$	1.0(4)
391.5(2)	4.0(7)	$(4_2^+) \rightarrow (2_2^+)$	0.9(4)
401.3(2)	5.5(7)	$(6_2^+) \rightarrow (4_2^+)$	1.1(3)
424.1(2)	4.2(5)	$(8_2^+) \rightarrow (6_2^+)$	1.5(1.0)
462.7(2)	3.9(5)	$(10_2^+) \rightarrow (8_2^+)$	—
507.6(3)	1.8(3)	$(12_2^+) \rightarrow (10_2^+)$	—
551.3(9)	0.5(3)	$(14_2^+) \rightarrow (12_2^+)$	—
674.5(6)	1.4(5)	$(4_2^+) \rightarrow 2_1^+$	—
414.5(5)	2.1(7)	$(4_2^+) \rightarrow 4_1^+$	—
478.8(2)	3.8(5)	$(6_2^+) \rightarrow 6_1^+$	0.6(3)
487.4(4)	2.3(6)	$(8_2^+) \rightarrow 8_1^+$	—

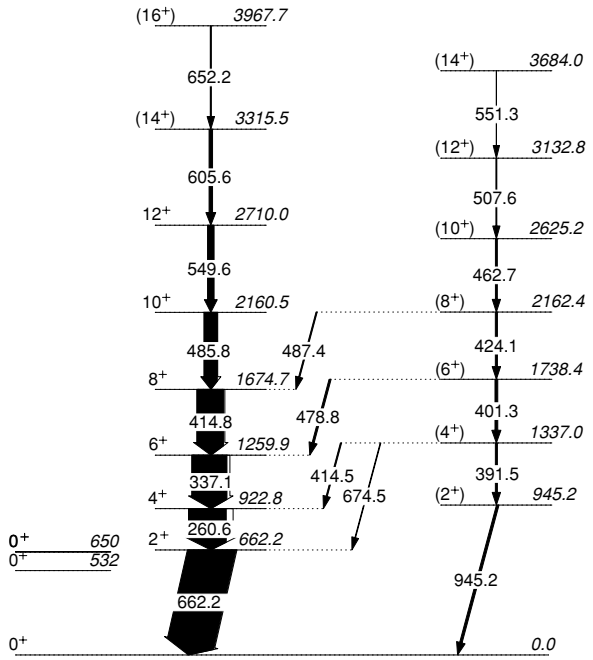

FIG. 3. Level scheme of ^{186}Pb deduced from the present data, including the two excited 0^+ states taken from Ref. [6]. The widths of the arrows are proportional to the measured intensities.

transition in ^{187}Tl a ratio of 1.2(2) was deduced, while for a dipole transition the corresponding value was 0.6(2).

The yrast $E2$ cascade in ^{186}Pb has recently been observed up to $I^\pi = 14^+$, where the $I^\pi = 12^+$ and $I^\pi = 14^+$ states are tentatively assigned [9]. In the present work, this cascade up to $I^\pi = 10^+$ is confirmed, and the 2710 keV level is assigned to $I^\pi = 12^+$, as the $12_1^+ \rightarrow 10_1^+$ transition has the angular distribution ratio of a stretched $E2$. Moreover, the coincidence data reveal candidates for the $14^+ \rightarrow 12^+$ and $16^+ \rightarrow 14^+$ transitions [Fig. 2(b)], the former having 4 keV higher energy than that reported in Ref. [8] and 10 keV higher than that reported in Ref. [9].

The 945 keV state, which de-excites to the ground state, is analogous to the 953 keV state in ^{188}Pb [15] and can be tentatively assigned as the 2_2^+ state. The 1337 keV level is tentatively assigned to $I^\pi = 4^+$ as it de-excites to the 2_1^+, 4_1^+ and 2_2^+ states. An $I = 3$ assignment is unlikely, as that would make the level highly nonyrast. For similar reasons the 1738 and 2162 keV levels are tentatively assigned to $I^\pi = 6_2^+$ and 8_2^+, respectively. The former assignment is in accord with the angular distribution information for the interband 479 keV transition, indicating its nonstretched $E2$ character.

Based on the coincidence relationships and intensity balance, the 463, 508, and 551 keV transitions are assumed to form an $E2$ cascade feeding the 8_2^+ state and thus, together with the 392, 401, and 424 keV transitions, a $K = 0$ band of $E2$ transitions. The 424 and 463 keV transitions could possibly correspond to the 425 and 464 keV transitions observed in Ref. [9].

It is intriguing to consider whether the newly observed band has characteristics that may be associated with oblate deformation.

First, a similar $K = 0$ side band built on top of a 2_2^+ state was observed in ^{188}Pb and associated with an oblate shape [15]. Unfortunately, owing to the dominant high-energy $E2(2_2^+ \rightarrow 0_1^+)$ ground-state transition and other overlapping transitions, the $E2(2_2^+ \rightarrow 0_2^+)$ transition to the band head as well as the possible branch to the 0_3^+ state from the 2_2^+ state remain unobserved in ^{188}Pb and in ^{186}Pb. In addition, the $2_2^+ \rightarrow 2_1^+$ transition was not observed in ^{186}Pb. The intensity limits still allow these transitions in ^{186}Pb to have $B(E2)$ values of 5, 25 and 30 times higher, respectively, than that for the $2_2^+ \rightarrow 0_1^+$ transition.

A remarkable feature of the side band in ^{186}Pb is the strong $I \rightarrow I$ and weak $I \rightarrow I - 2$ interband transitions to the prolate yrast band. The observed 674 keV branch from the 4_2^+ to the 2_1^+ state represents only about 3% of the $B(E2)$ value of the 392 keV intraband transition, whereas for the $4_2^+ \rightarrow 4_1^+$ 414.5 keV transition the corresponding value is 34%. The nonobservation of the other $I \rightarrow I - 2$ interband transitions allows intensity limits to be set. The upper limit for their $B(E2)$ values is determined to be 3% of that of the competing intraband transition.

If the new side band was a beta-vibrational band based on the prolate minimum, the competing $I \rightarrow I - 2$ and $I \rightarrow I$ $E2$ branches from the side band to the yrast band should, according to the Alaga rules [26], have similar $B(E2)$ values. Therefore, the $I \rightarrow I - 2$ transitions having the highest energy should be the dominant ones. This is clearly not what was

observed. Similar arguments make a gamma band an unlikely explanation for the observed band. However, such a γ band would presumably lie higher in energy and mix with the oblate band to some extent. This possibility has been discussed by Dracoulis *et al.* in ^{188}Pb, where a candidate for the odd-spin sequence of the γ band was observed [27].

The observed intensities for the $I \rightarrow I$ interband transitions from the 4_2^+, 6_2^+ and 8_2^+ states represent $B(E2)$ values, which are 20%–60% of those for the competing intraband transitions ($M1$-transitions of $\Delta I = 0$ between $K = 0$ bands are forbidden). The deduced intensity limits for the similar $I \rightarrow I$ transitions from the higher-lying states of the observed side band do not rule out the existence of $E2$ transitions of a similar strength. As pointed out in Ref. [15], the strong $I \rightarrow I$ interband transitions may be due to mixing of two different shapes.

The mixing of different shapes in heavy nuclei may result in considerable $E0$ components in $I \rightarrow I$ transitions. Based on the missing γ-ray intensities in coincidence gates, dominant $E0$ components were deduced in several interband $I \rightarrow I$ transitions in ^{188}Pb [15]. The present coincidence data for ^{186}Pb do not indicate any strong $E0$ components in the corresponding interband transitions within the statistical error bars. However, it should be noted that, because of the high energies of these transitions in ^{186}Pb compared with ^{188}Pb, possible $E0$ components of monopole strengths similar to those in ^{188}Pb may well be obscured by the much faster $E2$ components in ^{186}Pb.

Further support for association of the new side band with the 2p–2h structure can be found in mixing calculations. In a recent study that concentrated on describing intruder bands and configuration mixing, the nucleus ^{188}Pb was studied by using the algebraic formulation of the Interacting Boson Model (IBM). This approach allows the appearance of intruder states to be approximated by incorporating 2p–2h and 4p–4h excitations across the proton closed shell at $Z = 82$, next to the regular states of the 0p–0h configuration corresponding to the closed proton shell at $Z = 82$. For details on the choice of the parameters used within this approach, see Refs. [28] and [29].

Applying this description to the case of ^{186}Pb, two collective band structures result that can be associated mainly with 4p–4h and 2p–2h excitations. A detailed account of both the calculated energies of these bands and their electromagnetic properties will be presented in a forthcoming paper. Within the context of the present paper, the $B(E2)$ values for both intraband and interband transitions are shown, starting with the mainly 2p–2h band in Table II. The effective charges in the $E2$ transition operator were fitted to the two known $B(E2)$ values in ^{188}Pb [30]. The sequence of calculated $E2$ decays, starting from the higher spin states, allowed the construction of two collective bands. The excitation energies of the bands are in rather good agreement with the experimental values. The mixing amplitudes of the 0_2^+ and the 0_3^+ states are very similar to the results derived by Page *et al.* [31], although the mixing is somewhat more pronounced. It is clear from Table II that the calculated $I \rightarrow I - 2$ interband transitions are considerably weaker than the strong $I \rightarrow I$ interband transitions. These results are consistent with the observed experimental $E2$ branching, giving support to the idea that the side band is related more strongly to a microscopic 2p–2h structure.

TABLE II. Calculated $B(E2)$ values for transitions starting from the mainly 2p–2h band. Primes indicate an interband transition to the mainly 4p–4h band. The absence of primes denotes an intraband transition.

I_i	I_f	$B(E2)$ (W.u.)	I'_f	$B(E2)$ (W.u.)
14^+	12^+	190	$14'^+$	57
			$12'^+$	6
12^+	10^+	194	$12'^+$	41
			$10'^+$	3
10^+	8^+	194	$10'^+$	35
			$8'^+$	1
8^+	6^+	187	$8'^+$	34
			$6'^+$	<1
6^+	4^+	172	$6'^+$	37
			$4'^+$	!1
4^+	2^+	121	$4'^+$	50
			$2'^+$	!1
2^+	0^+	75	$2'^+$	83

The two constructed bands can now be linked with a collective interpretation by using a method to connect the IBM algebraic approach with a geometric collective rotational model analysis. The calculated IBM quadrupole moments were equated with the corresponding quadrupole moments of $K = 0$ bands. This allows an intrinsic quadrupole moment to be extracted within the collective rotational model for the two bands calculated within the IBM. For the band of the mainly 4p–4h configuration, corresponding to the experimental yrast band, this results in a positive sign, indicating prolate deformation. For the side band originating mainly from the 2p–2h configuration, a negative sign was obtained, indicating oblate deformation and supporting the present experimental results.

The kinematic moments of inertia ($\mathcal{J}^{(1)}$) for the observed candidate oblate band and the prolate yrast band in ^{186}Pb are plotted in Fig. 4. For comparison, values of $\mathcal{J}^{(1)}$ for the prolate bands in ^{182,184,188}Pb and oblate bands in ^{188,196}Pb are shown. Also included are the oblate bands based on a mainly proton 4p–2h shell-model configuration in ^{192}Po and ^{194}Po.

The $\mathcal{J}^{(1)}$ curves for the prolate bands in the even–even isotopes $^{182-188}$Pb are very similar (especially at high spin). The $\mathcal{J}^{(1)}$ values for the oblate bands are lower than those for the prolate bands, which is at least partially due to their small deformation. The curve for the candidate oblate band in ^{186}Pb differs from the others. It extends from small $\mathcal{J}^{(1)}$ values at low spin to values that are higher than those for the prolate bands. As shown in Fig. 4, similar behavior is also observed for the oblate band in ^{188}Pb, but starting at higher spin. It is difficult to associate this up-bend in ^{186}Pb with any alignment of valence nucleons, as it occurs at such low spin. Therefore it may be due to a shape change toward a more deformed oblate structure. Such structures are predicted to occur at relatively

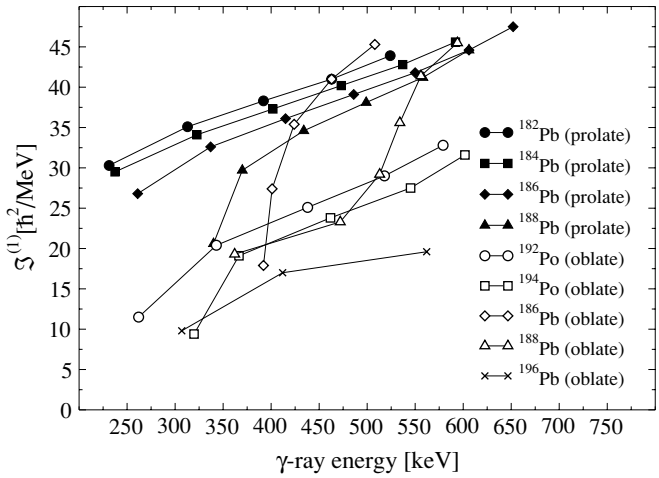

FIG. 4. Kinematic moment of inertia $\mathcal{J}^{(1)}$ as a function of γ-ray energy for the two collective bands in ^{186}Pb, together with those for known bands in nuclei close to ^{186}Pb. Data for other nuclei are taken from Refs. [5,15,32] and references therein.

low excitation energy in the even–even Pb isotopes close to the neutron midshell [33,34].

In summary, by employing an upgraded spectrometer system in a RDT measurement, high-quality in-beam $\gamma\gamma$ coincidence data for ^{186}Pb have been collected. A new low-lying side band has been identified. On the basis of observed strong $I \rightarrow I$ and weak $I \rightarrow I-2$ interband transitions to the prolate yrast band, this band is associated with an oblate shape. This interpretation is further supported by configuration mixing calculations within the interacting Boson model. The moment of inertia behavior of the new band may indicate a shape change toward a more deformed oblate shape.

This work has been supported by the EU-FP5-IHP-Access-to-JYFL Project (contract HPRI-CT-1999-00044), the EU-FP5-IHP-RTD-EXOTAG Project (contract HPRI-CT-1999-50017), by the Academy of Finland under the Finnish Centre of Excellence Programme 2000-2005 (project 44875) and by the EPSRC (UK). Financial support from the "FWO-Vlaanderen," the University of Ghent, as well as from the OSTC (Grant IUAP P5/07) is acknowledged (by V. Hellemans and K. Heyde). The UK/France (EPSRC/IN2P3) Loan Pool and EUROBALL Owners Committee is also acknowledged for the EUROGAM detectors of JUROGAM. This research was also supported through a European Community Marie Curie Fellowship.

[1] J. L. Wood, K. Heyde, W. Nazarewicz, M. Huyse, and P. Van Duppen, Phys. Rep. **215**, 101 (1992).
[2] P. Van Duppen, E. Coenen, K. Deneffe, M. Huyse, K. Heyde, and P. Van Isacker, Phys. Rev. Lett. **52**, 1974 (1984).
[3] P. Van Duppen, M. Huyse, K. Heyde, and J. L. Wood, J. Phys. G: Nucl. Part. Phys. **16**, 441 (1990).
[4] K. Heyde, J. Schietse, and C. De Coster, Phys. Rev. C **44**, 2216 (1991).
[5] R. Julin, K. Helariutta, and M. Muikku, J. Phys. G: Nucl. Part. Phys. **27**, 109(R) (2001).
[6] A. N. Andreyev *et al*., Nature (London) **405**, 430 (2000).
[7] J. Heese *et al*., Phys. Lett. **B302**, 390 (1993).
[8] A. M. Baxter *et al*., Phys. Rev. C **48**, R2140 (1993).
[9] W. Reviol *et al*., Phys. Rev. C **68**, 054317 (2003).
[10] D. G. Jenkins *et al*., Phys. Rev. C **62**, 021302(R) (2000).
[11] J. F. C. Cocks *et al*., Eur. Phys. J. **A3**, 17 (1998).
[12] K. Van de Vel *et al*., Eur. Phys. J. **A17**, 167 (2003).
[13] N. Bijnens *et al*., Z. Phys. A **356**, 3 (1996).
[14] J. Penninga *et al*., Nucl. Phys. **A471**, 535 (1987).
[15] G. D. Dracoulis *et al*., Phys. Rev. C **67**, 051301(R) (2003).
[16] R. S. Simon *et al*., Z. Phys. A **325**, 197 (1986).
[17] E. S. Paul *et al*., Phys. Rev. C **51**, 78 (1995).
[18] M. Leino *et al*., Nucl. Instrum. Methods Phys. Res. B **99**, 653 (1995).
[19] P. J. Nolan *et al*., Nucl. Phys. **A520**, 657c (1990).
[20] C. Rossi Alvarez, Nucl. Phys. News **3**(3), 10 (1993).
[21] R. D. Page *et al*., Nucl. Instrum. Methods Phys. Res. B **204**, 634 (2003).
[22] I. H. Lazarus *et al*., IEEE Trans. Nucl. Sci. **48**, 567 (2001).
[23] P. Rahkila, to be published.
[24] D. Radford (2000), http://radware.phy.ornl.gov/main.html
[25] J. Billowes, Hyperfine Interact. **30**, 265 (1986).
[26] G. Alaga, K. Alder, A. Bohr, and B. R. Mottelson, Dan. Vedensk. Setsk. Mat.-Fys. Medd. **29**(9), 1 (1955).
[27] G. D. Dracoulis *et al*., Phys. Rev. C **69**, 054318 (2004).
[28] V. Hellemans, R. Fossion, S. De Baerdemacker, and K. Heyde, Phys. Rev. C **71**, 034308 (2005).
[29] R. Fossion, K. Heyde, G. Thiamova, and P. van Isacker, Phys. Rev. C **67**, 024306 (2003).
[30] A. Dewald *et al*., Phys. Rev. C **68**, 034314 (2003).
[31] R. D. Page *et al*., in *Proceedings of the Third International Conference on Exotic Nuclei and Atomic Masses ENAM2001, Hämeenlinna, Finland, 2–7 July 2001*, edited by J. Äystö, P. Dendooven, A. Jokinen, and M. Leino (Springer-Verlag, Berlin, 2001), p. 309.
[32] J. R. Hughes *et al*., Phys. Rev. C **47**, 1337(R) (1993).
[33] W. Nazarewicz, Phys. Lett. **B305**, 195 (1993).
[34] M. Bender, P. Bonche, T. Duguet, and P.-H. Heenen, Phys. Rev. C **69**, 064303 (2004).